International Journal of General Medicine

Dovepress

open access to scientific and medical research

Open Access Full Text Article

ORIGINAL RESEARCH

Three-Dimensional Heat Map: The OTA/AO Type 43C Pilon Fracture Lines Distribution

Yuling Gao[1], Yanrui Zhao[1], Hanzhou Wang[1], Xiaopei Xu[1], Zhexian Cheng[2], Tianchao Lu[1], Junlin Zhou[1], Yang Liu[1]

[1]Orthopedics Department, Affiliated Beijing Chaoyang Hospital of Capital Medical University, Bejing, People's Republic of China; [2]Preventive Dentistry Department, Affiliated Stomatology Hospital of Guangzhou Medical University, Guangzhou, Guangdong Province, People's Republic of China

Correspondence: Junlin Zhou; Yang Liu, Beijing Chaoyang Hospital, Capital Medical University, Gongtinan Road 8#, Beijing, 100020, People's Republic of China, Email junlinzhou_article@outlook.com; y0ring1996@163.com

Background: This study aimed to create three-dimensional heat map and study the characteristic of fracture lines and represented fragments of OTA/AO type 43C pilon fractures.

Methods: CT scan was performed in105 fractures diagnosed with OTA/AO type 43C pilon fractures between January 2017 and December 2022. Three-dimensional pilon fracture maps were created and converted into fracture heat maps. CT scan graphic parameters including the fracture line height, α angle, β angle, the ratio of the area and size of bone fragment represented by the fracture line to the total articular surface were measured.

Results: The study included 105 patients with 91 males and 14 females. The fractures included C1 (n=16), C2 (n=23), and C3 (n=66). There was no statistically different among the most parameters except in the fracture-line height of the anterior fracture line (p=0.03) and the sagittal fracture line (p=0.02) between C2 and C3 pilon fractures. The average size of the anterolateral fragment, occupied approximately 13.5% of the articular surface area, was (11.5±2.8) mm × (20.5±6.3) mm with the average height of 29.8 mm. The average size of the posterolateral fragment, occupied approximately 13.0% of the articular surface area, was (15.7±4.6) mm × (19.3 ±4.0) mm with the average height of 19.1 mm.

Conclusion: This study demonstrates that the articular surface fracture lines in the C type pilon fracture are formed by fixed main fracture lines. The understand of morphological and distribution characteristics of the fracture lines and size of fragments in OTA/AO type 43C pilon fractures would help the surgeons take suitable approach and fixation.

Keywords: pilon fractures, heat map, three-dimensional reconstruction, classification

Introduction

Pilon fractures account for 10% of lower extremity fractures and are challenging to treat,[1] which are caused by an axial high-energy impact on the distal tibial plafond, resulting in complex fractures and severe soft tissue injuries.[2,3] For the present, AO/OTA (Arbeitsgemeinschaft für Osteosynthesefragen/Orthopaedic Trauma Association) classification is the most widely used classification to date, which is divided into 3 types: A type extra-articular, B type partial articular, and C type total articular. Pilon fractures are defined as distal tibia fractures with joint involvement and refer to type AO/OTA 43B and 43C.[4]

Caused by high-energy violence, usually involving intra-articular comminution fractures, type AO/OTA 43C pilon fractures are common. It is crucial to understand the pattern of pilon fractures so as to choose the appropriate approach and fixation for the treatment. Computed tomography (CT) scans and fracture map are widely used. Topliss et al[5] observed 108 CT scans of pilon fractures and proposed six fragments of the articular surface. Cole et al[6] related the fracture to classification and mapped 38 consecutive-type AO/OTA 43C3 pilon fractures by using axial CT scan. They proposed that AO/OTA type 43C3 pilon fractures could be defined as 3 main fragments: anterior, medial, and posterior fragments and illustrated that more than 90% of the major fracture lines occurred in the "corridors". However, Cole's study was qualitative description. The quantitative research on the fracture lines are lack and the other C type pilon fractures are neglected. This retrospective study aimed to create 3D heat maps of AO/OTA type 43C pilon fractures and study the morphological characteristic of fracture lines and represented fragments.

Received: 19 October 2023
Accepted: 17 January 2024
Published: 30 January 2024

Materials and Methods

We retrospectively reviewed 105 patients diagnosed with C type pilon fractures between January 2017 and December 2022. We use the data obtained from the subjects to conduct a retrospective analysis. All patients underwent CT scans. The diagnosis of a pilon fracture was established based on distal tibia metaphysis fractures involving the articular surface to the definition. Based on the AO/OTA classification, C type pilon fractures were divided into 3 subtypes (C1, simple fractures of complete articular surfaces and metaphysis; C2, simple fractures of complete articular surfaces with metaphyseal comminuted fractures; C3, comminuted fractures of articular surfaces). The present study was granted approval by the Medical Ethics Committee of Beijing Chaoyang Hospital, and the imaging material data adhered to the ethical standards outlined in the 1964 Declaration of Helsinki. Informed consent was obtained from all participants and their legal guardian(s) for the participants of age 18. All methods were performed in accordance with the relevant guidelines and regulations.

The inclusion criteria for the study were as follows: (1) pilon fractures; (2) patients aged 18 years or older, regardless of sex and medical history; (3) unilateral or bilateral fractures; and (4) fresh fractures within 3 weeks after injury. The exclusion criteria included pathological fractures and secondary fractures. One senior radiologist and two senior orthopaedic surgeons reviewed all images.

Mapping 3D Fracture Lines

All data from CT scans were exported in DICOM format to create 3D models using the Mimics 21.0 system (Materialise, Belgium). The fractures were simultaneously reduced in the viewport. The reset 3D models were imported into 3-matic research 13.0 (Materialise, Belgium) software for rotation, mirror flipping, and dimension normalization. This procedure allowed us to locate, coincide and superimpose 3D fracture lines on standard 3D tibial models. Each fracture line was drawn using a curve create tool in 3-matic research. The models were then converted into fracture heat maps.

Converting 3D Fracture Lines Map to Heat Map

Open Python (python 3.10) and Create a binary bone fracture line, which is convenient for drawing to confirm that the deep color is the dense fracture area. 1. The fracture map was preliminarily processed with Photoshop to increase the contrast between the fracture line and the background as much as possible. 2. OpenCV (OpenCV 2.2.0) was used to read the fracture line preliminarily processed by Photoshop, and a reasonable threshold was selected to binarize the fracture line with the background, so as to ensure that 0 was the background and 1 was the fracture as much as possible. 3. The linear fracture density was quantified by arithmetic average, that is, the arithmetic average of matrix elements in a certain range around a pixel was selected as the linear fracture density value of the point. Fracture line density was color-coded from blue (low density) to deep red (high density) 4. The linear density matrices of the fractures that had been quantified were plotted using matplotlib (Figure 1).

Statistical Analysis

Statistical analysis was performed using SPSS version 22.0 (SPSS Inc, Chicago, Illinois, USA). Statistical information of general information of patients was conducted by using single sample K–S test and run test to test the normal distribution. The data in each group presented non-normal distribution with unequal variances were expressed as a median (min, max). The p values of each group were adjusted by means of independent samples t -test to do the test. p <0.05 was considered statistically significant.

Measures and Parameters

After the actual area of fracture fragment in CT transverse section was measured by Mimics21.0 software in each case, the CT slice with the largest measured value was selected as the study slice, and the following characteristic of fracture lines and the fragments represented were measured.

1. It is defined as angle α that the angle between the sagittal fracture line and the ankle mortise line (Figure 2); 2. It is defined as angle β that the angle between the fracture line of the transverse section and the line of the bilateral malleolus which was taken as the axis of the maximum tibiofibular notch connection (Figure 3); 3. Height of collapse of the distal tibial articular surface and height of the metaphyseal fracture line; 4. The ratio of the area of bone fragment represented by the fracture line to the total articular surface area were measured; 5. The size of the anterolateral and the posterolateral fragments was measured.

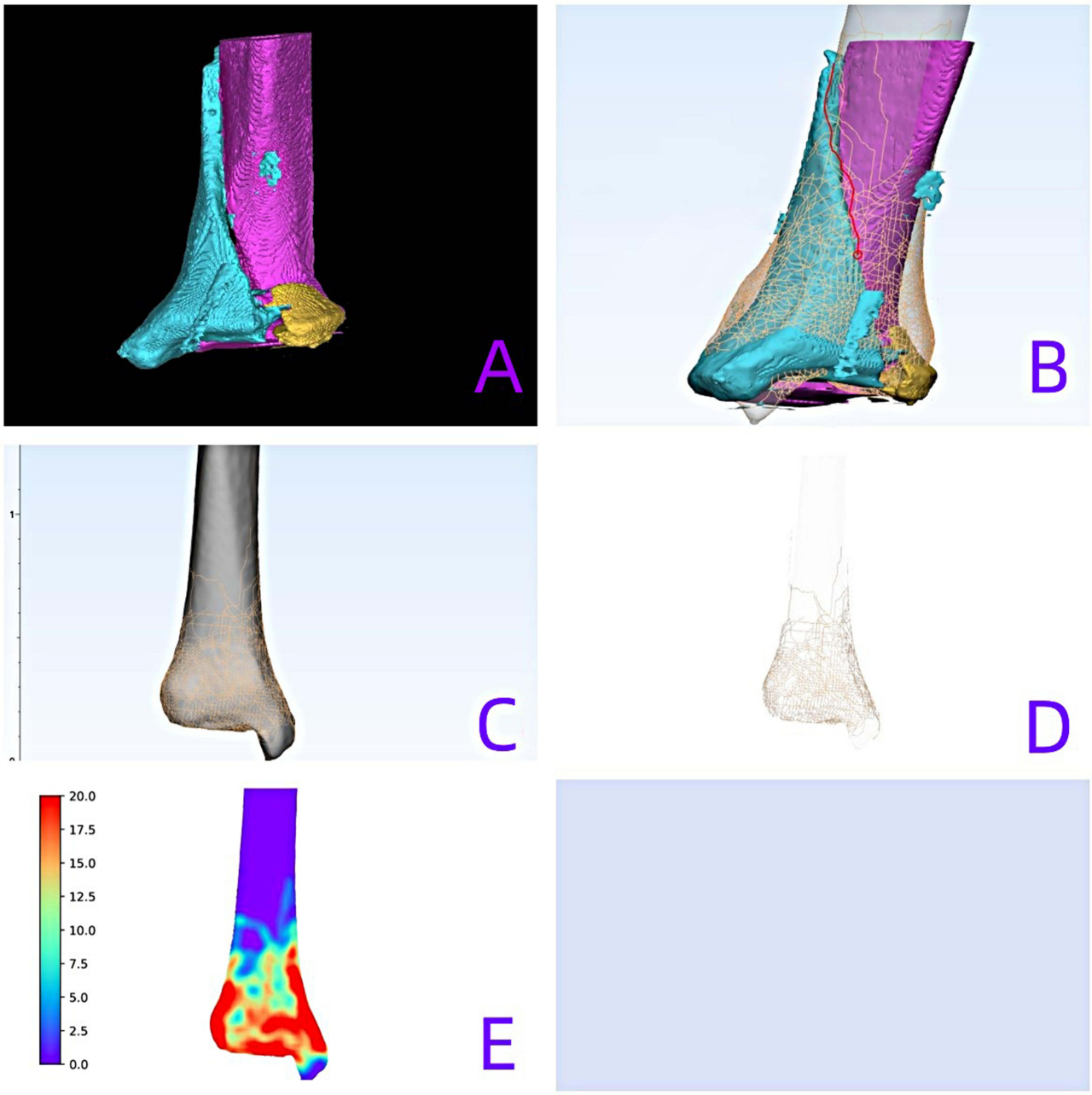

Figure 1 (**A**) Creating and reducing 3D fracture models using the Mimics 21.0 system; (**B**) Drawing fracture line on the standard right tibial model in 3-matic research; (**C**) Superimposing 3D fracture lines on standard 3D tibial models; (**D**) Abstracting the fracture lines through Photoshop; (**E**) Converting fracture lines map to heat map by using Python.

Results

Patient demographics and fracture heat maps

The study included 105 pilon fractures with 91 males and 14 females. The fractures included C1 type (n=16), C2 type (n=23), and C3 type (n=66) (Table 1).

The characteristic of C1 pilon fracture lines distribution are shown in Figure 4. The metaphyseal fracture lines of the C1 pilon fractures encircled the distal tibia, and the simple articular fracture lines divided the distal tibia into two parts. The articular fracture lines mainly included the anterior fracture lines (the AFLs, the fracture lines between the fibular notch and the bulk of the anterior tibial articular surface), the posterior fracture lines (the PFLs, the fracture lines between the fibular notch and the bulk of the posterior tibial articular surface), the anterolateral fracture lines (the ALFLs, the fracture lines extending from the fibular notch to the anterior surface less than 50% of the width of the distal tibial

Figure 2 The angle α is defined that the angle between the sagittal fracture line and the ankle mortise line.

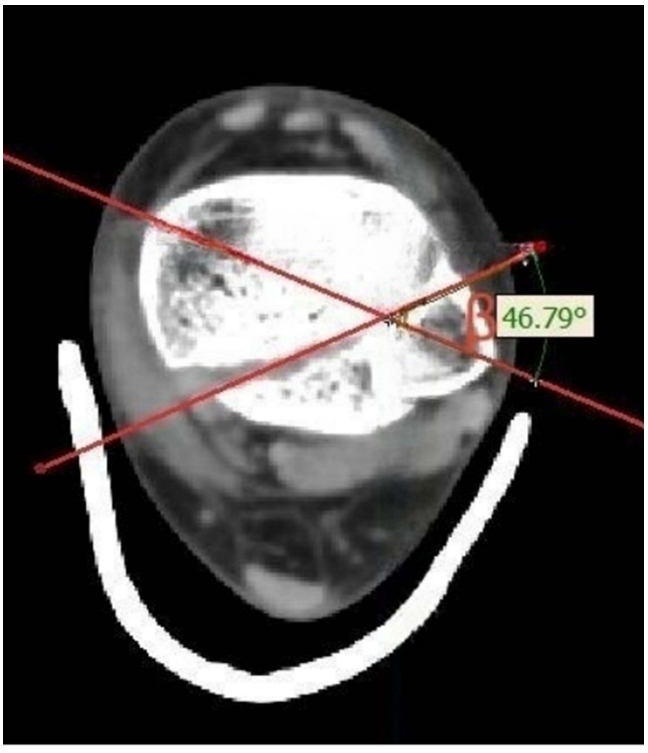

Figure 3 The angle β is defined that the angle between the fracture line of the transverse section and the line of the bilateral malleolus which was taken as the axis of the maximum tibiofibular notch connection.

plafond) and the sagittal fracture lines (the SFLs). Based on the fracture lines, four main types of fragments were identified: anterolateral fragments, posterior fragments, anterior fragments, and medial fragments. The characteristics of the C1 pilon fracture lines are recorded in Table 2.

Table 1 The General Information of the Patients (n=105)

Fracture Type	C1	C2	C3
Patient Number	16	23	66
Age(year)	46.8 (23–71)	50.5 (28–70)	42.4 (15–71)
Sex (Male: Female)	12:4	19:4	60:6
Side (Left: Right)	9:7	8:11	23:43

C2 type fractures were simple joint fractures with multiple bone fragments in the metaphysis (Figure 5). A total of 23 cases were included in this study. The comminuted areas of the metaphyseal fractures were mainly concentrated in the proximal medial malleolus and the distal tibia anterolateral region. The articular surface fracture lines were formed by the SFLs, the AFLs, ALFLs and PFLs. The characteristics of the C2 pilon fracture lines were recorded in Table 3.

For a type C3 pilon fracture, as shown in Figure 6, the distal articular surface of the tibia is typically affected except for sparse fracture lines at the medial malleolus and posterolateral articular plafond. It is found that T shape fracture lines, V shape fracture lines and Y shape fracture lines. These fracture lines were simplified as the combination of AFLs, ALFLs, PFLs and SFLs. The characteristics of the C3 pilon fracture lines are recorded in Table 4.

The fracture lines and represented fragments characteristics in three C types pilon fracture were compared (Tables 5–7). There were no statistically different among most parameters. However, when comparing C2 and C3 pilon fractures, there was a statistically significant difference in the height of the AFLs (p=0.03) and the SFLs (p=0.02). The height of the fracture lines in C2 pilon fractures was greater than that in C3 pilon fractures.

In this study, the average size of the anterolateral fragment was (11.5±2.8) mm × (20.5±6.3) mm with the average height of 29.8 mm (range from 16.0 to 66.0 mm), which occupied approximately 13.5% of the total articular surface of the tibial plafond. Additionally, the posterolateral fracture line (the PLFL, the fracture line extending from the fibular notch to the posterior surface less than 50% of the width of the distal tibial plafond) was found in some type C3 pilon fractures. The average size of the posterolateral fragment was (15.7±4.6) mm × (19.3±4.0) mm with the average height of 19.1 mm (range from 10.2 to 26.7 mm), which occupied approximately 13.0% of the total articular surface of the tibial plafond.

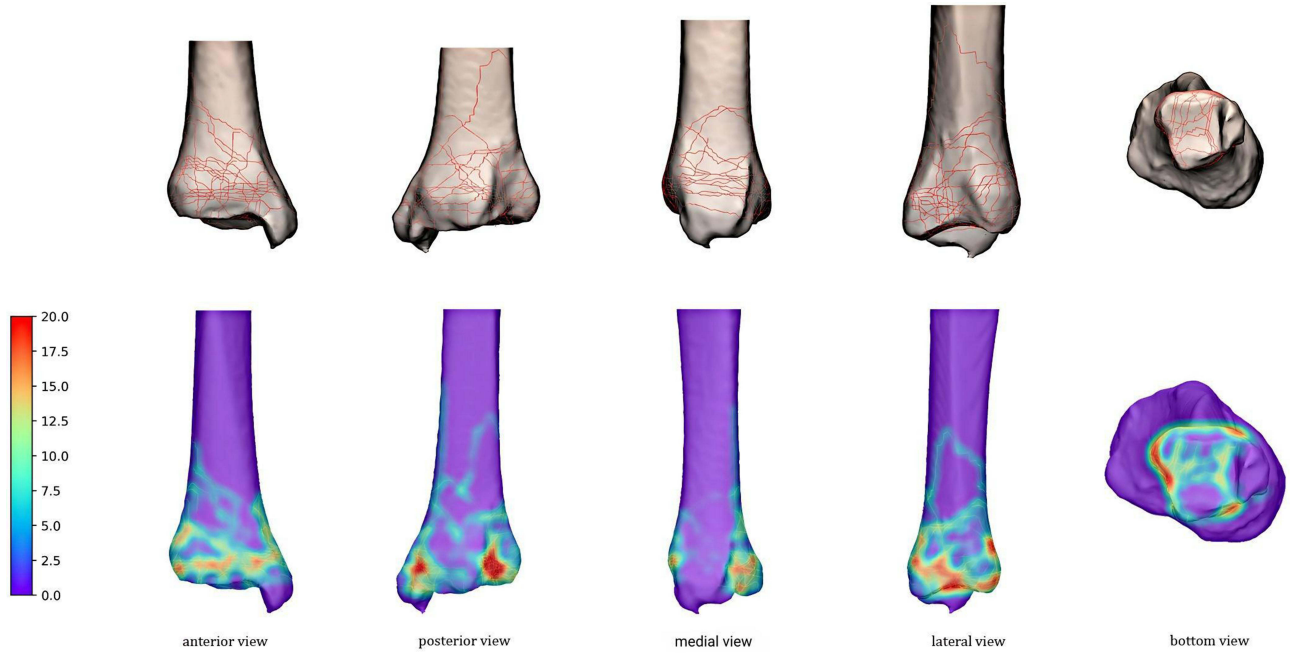

Figure 4 In C1 pilon fracture, the metaphyseal fracture lines of the C1 pilon fractures encircled the distal tibia, and the simple articular fracture lines, including anterior fracture lines, the posterior fracture lines, the anterolateral fracture lines and the sagittal fracture lines, divided the distal tibia into two parts.

Table 2 The Characteristic of the C1 Pilon Fracture Lines

Fracture Lines Type	Fracture Lines Number	Angle α(°)	Height(mm)	Angle β(°)	Ratio(%)
AFL[a]	3	37.7 (34.0, 39.1)	41.9 (23.3, 60.1)	33.3 (0, 36.5)	36.2 (16.2, 37.8)
PFL	5	58.8±18.0	24.4±7.5	33.4±5.0	28.8±7.2
ALFL	5	65.6±14.6	31.1±10.0	39.0±15.9	17.4±5.8
SFL[a]	3	68.2 (57.2–79.1)	32.4 (29.1, 35.6)	84.5 (77.2, 91.8)	27.0 (21.7, 32.2)

Notes: [a]The data in the AFL group and the SFL presented non-normal distribution with unequal variances and were expressed as a median (min, max).
Abbreviations: AFL, anterior fracture line; PFL, posterior fracture line; ALFL, anterolateral fracture line; SFL, sagittal fracture line.

Discussion

In the current study, we described the distribution of OTA/AO type 43C pilon fracture lines and analyzed their morphological characteristics. The common pilon fracture lines are formed by AFL, PFL, ALFL, and SFL, with particular attention given to PLFL in type 43C3 pilon fractures.

Due to the extensive injury to the distal tibia's surface, orthopedic surgeons face challenges in comprehending and treating pilon fractures due to their complex articular and comminuted metaphyseal fractures. Rüedi and Allgöwer[7] provided a useful and simple classification with a relative high reliability, but could not help the surgeon to understand the fracture pattern such as the distribution of fracture lines. Topliss[5] and Leonetti[8] separately proposed their new classifications based on CT scan to study the joint morphology of pilon fractures. However, the authors did not breakdown the articular fracture pattern with respect to a classification system. For the present, the AO/OTA classification[9] which includes 6 types and 18 subtypes is the most comprehensive and systemic pilon fractures classification till now and the AO/OTA type C is the most complex type of pilon fracture. In this study, each subtype in AO/OTA type C pilon fractures is analysed and summarized. CT scan has been proved to be effective in identifying the morphology of fracture fragments and fracture lines, which would effect the treatment plan. Cole et al[6] drew a fracture map of type C3 pilon fracture based on the AO/OTA classification. They also found a fracture extended from the fibular notch to the anterior and posterior aspects of the medial malleolus, and comminuted fractures occurred primarily in the anterolateral region. As a result, the fracture lines formed a Y-shaped corridor where more than 90% of the major fracture lines occurred. Likenessly in our study, we also found the main fracture lines derived from the fibular notch to the

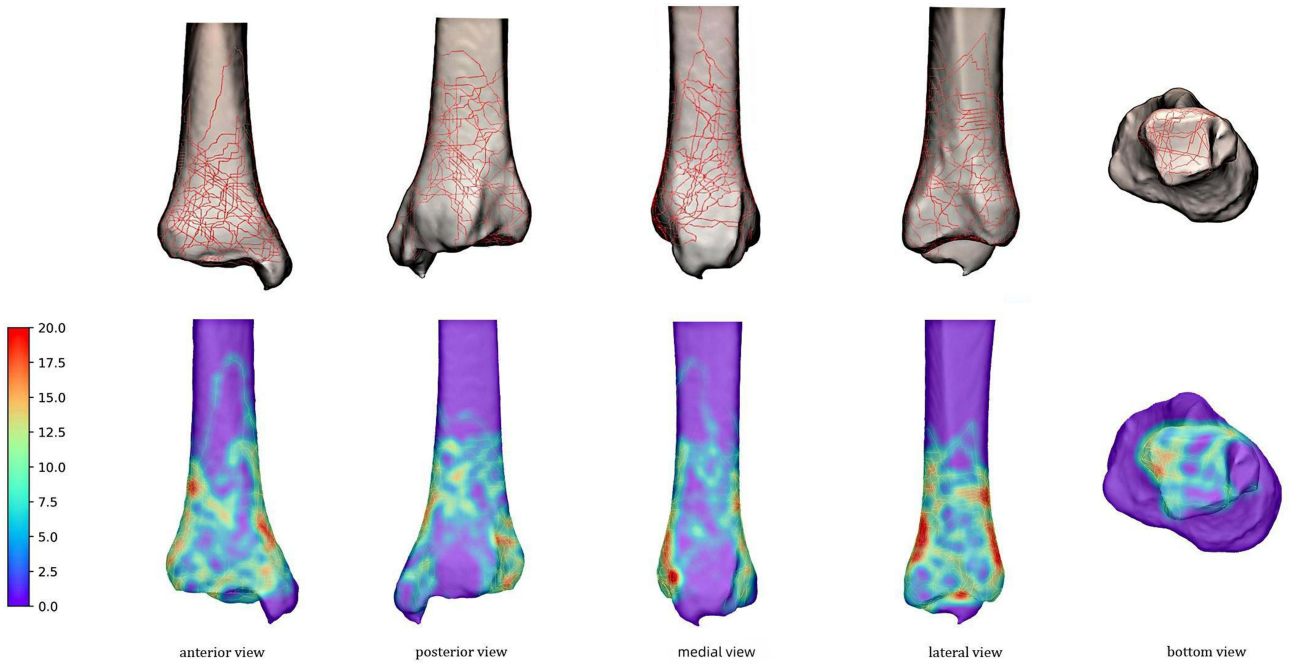

Figure 5 In C2 pilon fracture, fractures were simple joint fractures with multiple bone fragments in the metaphysis.The comminuted areas of the metaphyseal fractures were mainly concentrated in the anteromedial and the anterolateral distal tibia.

Table 3 The Characteristic of the C2 Pilon Fracture Lines

Fracture Lines Type	Fracture Lines Number	Angle α(°)	Height(mm)	Angle β(°)	Ratio(%)
AFL	6	55.2±12.7	51.4±11.3	19.5±16.4	28.2±12.7
PFL	5	60.0±10.4	41.8±13.6	33.2±9.8	35.0±10.9
ALFL	7	71.3±7.0	44.1±21.0	55.4±9.5	20.1±6.2
SFL	5	57.9±12.1	40.7±9.8	64.6±13.7	35.1±10.5

Abbreviations: AFL, anterior fracture line; PFL, posterior fracture line; ALFL, anterolateral fracture line; SFL, sagittal fracture line.

anterior margin of medial malleolus or the posterior margin of medial malleolus (malleolus sulcus area). In addition, the ALFLs, the PLFLs and the SFLs are depicted in this study. Majority of the SFLs cross the junction area between the articular surface and the medial malleolus. Different from Cole's qualitative description, this study does quantitative research on the fracture lines and represented fragments. Except for the height of the anterior fragment and the sagittal fragment, which are greater in C2 type pilon fractures compared to C3 pilon fractures, there are no differences in relative characteristic parameters among the other main fracture lines and represented fragment. Therefore in C-type fracture, the distal tibia articular fracture lines are formed by fixed main fracture lines, which would help the surgeons take suitable angle and length of screws for fixation. The fixed main fracture lines may also indicate the existence of fixed fracture patterns and are caused by a combination of talus impaction force and ligamentous stretching force. Based on the quantitative characteristics of fracture lines, it is hypothesized that the anterior talofibular ligament stretching affects the ALFL, while the deltoid ligament affects the SFL, and the posterior intermalleolar ligament affects the PFL. Additionally, it is suggested that the posterior inferior tibiofibular ligament may affect the PLFL.

The choice of surgical approach for pilon fracture is closely related to the pilon fracture pattern and reduction strategy.[1,10–12] The aims of treatment of pilon fractures are restoring the articular surface and distal tibial alignment anatomically and preserving the tenuous soft tissue envelope.[2] The common approaches, such as the anteromedial approach, the anterolateral approach and the posterolateral approach, are widely used.[13] Tang et al[14] proposed a four-column division of the distal tibia and advocated for fixation of each fractured column, necessitating the utilization of combination approaches. However, it should be noted that employing a combination of approaches in complex pilon

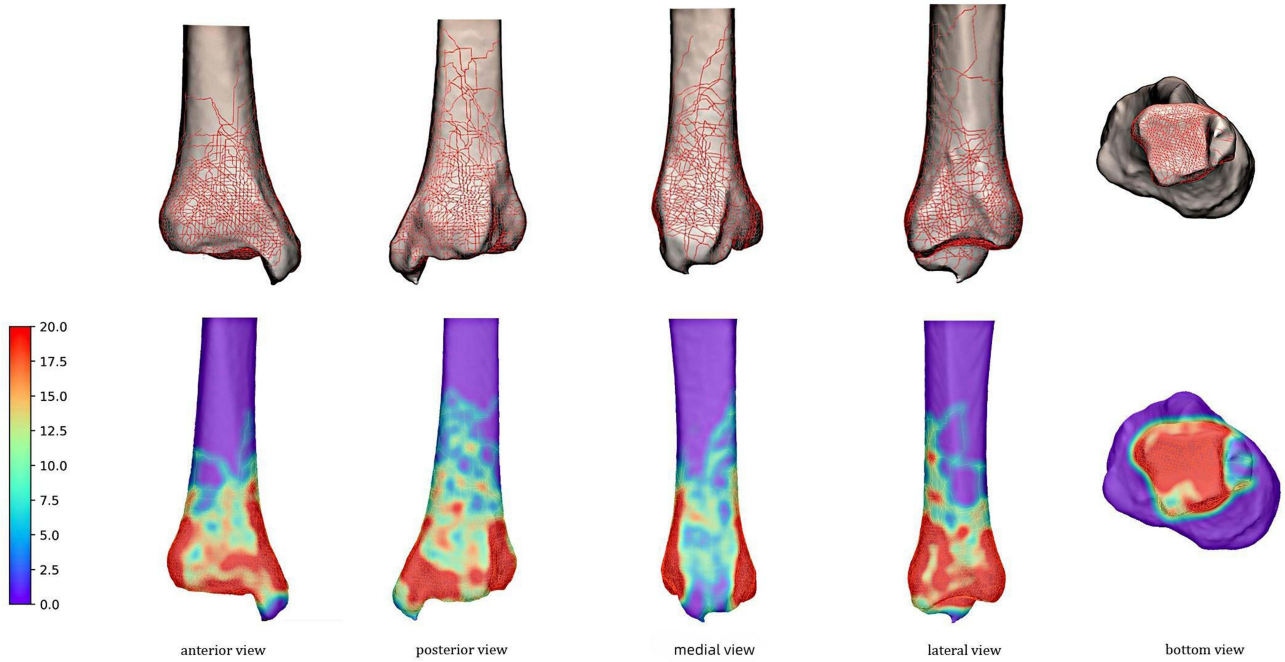

Figure 6 In C3 pilon fracture, the distal articular surface of the tibia was basically involved except the fracture line at the medial malleolus, the anterolateral articular plafond and the posterolateral articular plafond were sparsely distributed.

Table 4 The Characteristic of the C3 Pilon Fracture

Fracture Lines Type	Fracture Lines Number	Angle α(°)	Height(mm)	Angle β(°)	Ratio(%)
AFL	49	53.6±15.3	31.5±15.0	17.4±14.5	28.0±5.4
PFL	56	54.6±19.1	27.4±19.0	22.1±19.4	31.9±8.2
ALFL	35	61.6±14.0	30.7±14.5	46.2±20.3	13.5±5.7
SFL	61	61.0±11.9	26.2±10.6	73.8±15.1	31.6±7.2

Abbreviations: AFL, anterior fracture line; PFL, posterior fracture line; ALFL, anterolateral fracture line; SFL, sagittal fracture line.

Table 5 The Comparison of C1 and C2 Pilon Fracture Lines

	C1	C2	*p*
Angle α(°)			
ALFL	65.6±14.6	71.3±7.0	0.46
PFL	58.8±18.0	60.0±10.4	0.35
AFL	37.7 (34.0, 39.1)	55.2±12.7	–
SFL	68.2 (57.2, 79.1)	57.9±12.1	–
Height(mm)			
ALFL	31.1±10.0	44.1±21.0	0.26
PFL	24.4±7.5	41.8±13.6	0.07
AFL	41.9 (23.3, 60.1)	51.4±11.3	–
SFL	32.3 (29.1, 35.6)	40.7±9.8	–
Angle β(°)			
ALFL	39.0±15.9	55.4±9.5	0.08
PFL	33.4±5.0	33.2±9.8	0.41
AFL	33.3 (0, 36.5)	19.5±16.4	–
SFL	84.5 (77.2, 91.8)	64.6±13.7	–
Ratio(%)			
ALFL	17.4±5.8	20.1±6.2	0.50
PFL	28.8±7.2	35.0±10.9	0.19
AFL	36.2 (16.2, 37.8)	28.2±12.7	–
SFL	27.0 (21.7, 32.2)	35.1±10.5	–

Notes: – The sample size was insufficient for statistical analysis.
Abbreviations: AFL, anterior fracture line; PFL, posterior fracture line; ALFL, anterolateral fracture line; SFL, sagittal fracture line.

Table 6 The Comparison of C1 and C3 Pilon Fracture Lines

	C1	C3	*p*
Angle α(°)			
ALFL	65.6±14.6	61.6±14.0	0.60
PFL	58.8±18.0	54.6±19.1	0.73
AFL	37.7 (34.0, 39.1)	53.6±15.3	–
SFL	68.2 (57.2, 79.1)	61.0±11.9	–
Height(mm)			
ALFL	31.1±10.0	30.7±14.5	0.96
PFL	24.4±7.5	27.4±19.0	0.97
AFL	41.9 (23.3, 60.1)	31.5±15.0	–
SFL	32.3 (29.1, 35.6)	26.2±10.6	–

(*Continued*)

Table 6 (Continued).

	C1	C3	*p*
Angle β(°)			
ALFL	39.0±15.9	46.2±20.3	0.50
PFL	33.4±5.0	22.1±19.4	0.20
AFL	33.3 (0, 36.5)	17.4±14.5	–
SFL	84.5 (77.2, 91.8)	73.8±15.1	–
Ratio(%)			
ALFL	17.4±5.8	13.5±5.7	0.23
PFL	28.8±7.2	31.9±8.2	0.28
AFL	36.2 (16.2, 37.8)	28.0±5.4	–
SFL	27.0 (21.7, 32.2)	31.6±7.2	–

Note: – The sample size was insufficient for statistical analysis.
Abbreviations: AFL, anterior fracture line; PFL, posterior fracture line; ALFL, anterolateral fracture line; SFL, sagittal fracture line.

Table 7 The Comparison of C2 and C3 Pilon Fracture Lines

	C2	C3	*p*
Angle α(°)			
ALFL	71.3±7.0	61.6±14.0	0.09
PFL	60.0±10.4	54.6±19.1	0.58
AFL	55.2±12.7	53.6±15.3	0.85
SFL	57.9±12.1	61.0±11.9	0.63
Height(mm)			
ALFL	44.1±21.0	30.7±14.5	0.16
PFL	41.8±13.6	27.4±19.0	0.18
AFL	51.4±11.3	31.5±15.0	0.03*
SFL	40.7±9.8	26.2±10.6	0.02*
Angle β(°)			
ALFL	55.4±9.5	46.2±20.3	0.36
PFL	33.2±9.8	22.1±19.4	0.43
AFL	19.5±16.4	17.4±14.5	0.81
SFL	64.6±13.7	73.8±15.1	0.27
Ratio(%)			
ALFL	20.1±6.2	13.5±5.7	0.09
PFL	35.0±10.9	31.9±8.2	0.59
AFL	28.2±12.7	28.0±5.4	0.99
SFL	35.1±10.5	31.6±7.2	0.46

Notes: *$p<0.05$ There is a statistical difference in the characteristics of fracture lines between the two types of pilon fractures.
Abbreviations: AFL, the anterior fracture line; PFL, the posterior fracture line; ALFL, the anterolateral fracture line; SFL, the sagittal fracture line.

fractures involving multiple columns may lead to an increased incidence of complications.[15,16] Bakan et al[17] further suggested that proper placement of a distal tibial medial anatomical plate can effectively address anterior and posterior column fractures, while screws inserted through an anterolateral plate can partially stabilize the medial column. Our study on the type 43C pilon fracture serves as a valuable reference for guiding the optimal selection of surgical approaches. Type C1 pilon fractures can be divided into three subtypes and treated through single approach.[9] For C1.1 fractures (without impaction) and C1.3 fractures (extending into the diaphysis), the placement of the main plate is contingent upon the injury mechanism and fracture-line height, with a preference for either an anterolateral or medial approach. For C1.2 fractures (with impaction), due to the necessary of reducing impaction articular surface, an anteromedial approach is needed and an anterior locking plate is placed. The distribution of fracture lines in C2 type

fractures is similar to that of C1, except for the presence of higher fracture lines and a multifragmentary metaphyseal fracture. According to our study, the multifragmentary sites are mainly concentrated in the anteromedial and the anterolateral distal tibia. Consequently, the main plate is recommended to be placed covering the multifragmentary site through the anteromedial approach or the anterolateral approach.

For C3 fracture, the distal articular surface of the tibia was basically involved except the fracture line at the medial malleolus, the anterolateral articular plafond and the posterolateral articular plafond were sparsely distributed. It demands that not only the main fragments, anterior, medial and posterior fragments, are need to be fixed, but also the small fragments like the anterolateral fragments and posterolateral fragments should not be missed. Although the current screw trajectory of ten commercially available distal tibia plates could capture the majority fragments, the medial fragment, the anterolateral fragment also named Tillaux-Chaput fragment and the Volkmann fragment may be missed by a single plate.[1] Sohn et al[18] emphasized that anatomical distal tibial locked plates are unable to adequately secure the anterolateral fragment when the sagittal height is less than 14.85 mm or the medial-lateral distance is <15.02 mm. In this study, the anterolateral fragment measured (11.5±2.8) mm×(20.5±6.3) mm with a height ranging from 16.0 mm to 66.0 mm, accounting for 13.5% of the articular surface area, thus supporting the preference for utilizing an anterolateral approach in fixing this fragment. From the bottom view of the C3 pilon fracture heat map in this study, the density of fracture lines in the posterolateral part of the distal tibia articular surface is few and scattered. The form of the posterolateral fragment has been described in several studies. Mason[19] and Vosoughi[20] proposed that pilon subtypes occur when the talus rotates and impacts the posterolateral corner of the tibia, forming posterolateral fragments. A biomechanical study on posterior malleolar fractures conducted by Haraguchi and Armiger indicated that the posterolateral fragment is considered an avulsion caused by tension from the posterior inferior tibiofibular ligament.[21] The posterior column serves as a crucial reference for reducing pilon fractures, acting as the "keystone" of the entire articular surface reduction.[22] Even though the indirect strategies for reducing the posterior fragments through either the anterior approach or percutaneous accessory incisions have been developed, the use of combined anterior and posterior approach is a better option for open reduction of the posterior column in direct view.[4] Based on our surgical experience, the posterolateral approach is the only way to directly expose the posterolateral fragments, considering that they account for 13.0% of the total articular surface of the tibial plafond in our study. Based on our surgical experience, we produced a flow chart regarding the selection of surgical approaches for type C pilon fractures (Figure 7).

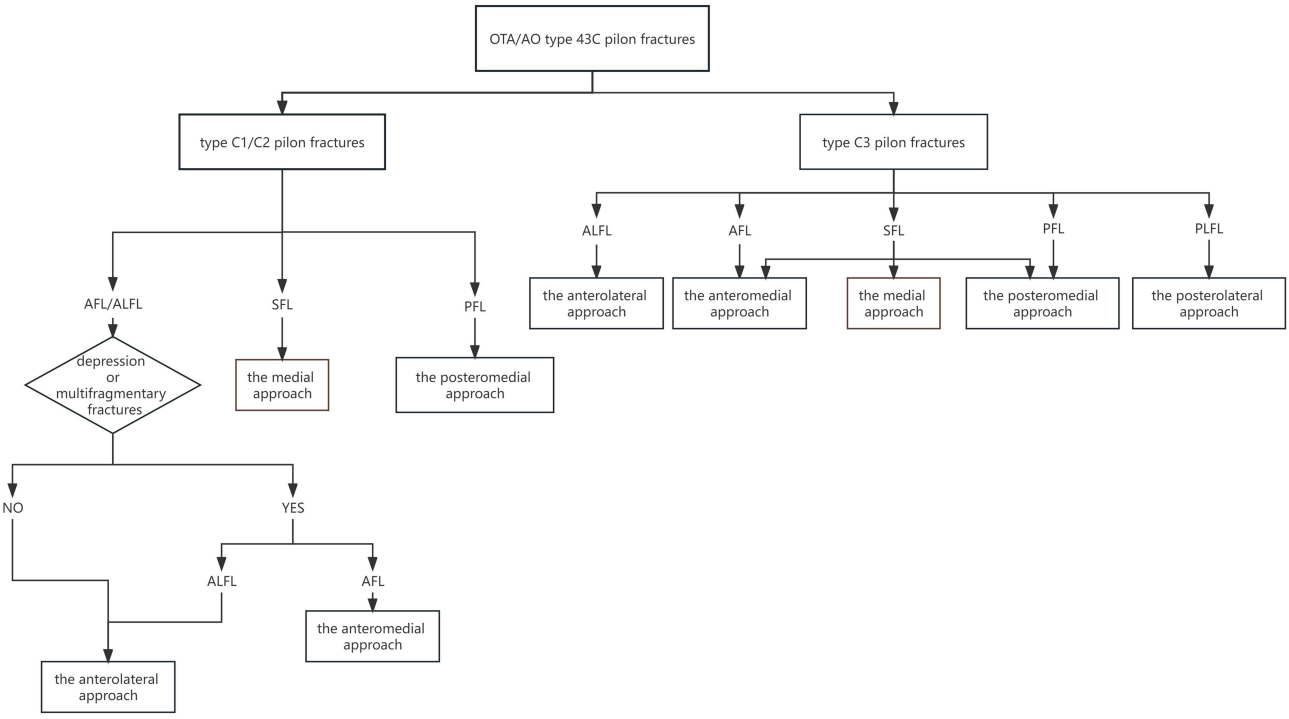

Figure 7 Selection of surgical approaches for type C pilon fractures. The approach for the SFLs can be determined by the surgeon's experience, with three different approaches available. AFL, anterior fracture line; PFL, posterior fracture line; ALFL, anterolateral fracture line; SFL, sagittal fracture line; PLFL, posterolateral fracture line.

The deficiency of this study is that the standard tibial model of three-dimensional reconstruction does not take into account the morphological differences of different fracture individuals. The limited number of patients included in this study may affect the outcome. Increasing the sample size may better represent the characteristic of fracture lines and fragments. Due to the small sample of C1 pilon fracture, this study lacks the comparison of fracture lines between C1 and other C-type pilon fracture lines. The PLFL needs to be studied in other C-type pilon fracture. At last, the parameters for the small fragments in CT evaluation may have poor precision may not represent actual numerical values of the fragments.

Conclusion

This study demonstrates that the articular surface fracture lines in the C-type pilon fracture are formed by fixed main fracture lines. The understand of morphological and distribution characteristics of the fracture lines and size of fragments in OTA/AO type 43C pilon fractures would help the surgeons take suitable approach and fixation.

Ethics Approval

The present study was granted approval by the Medical Ethics Committee of Beijing Chaoyang Hospital, and the imaging material data adhered to the ethical standards outlined in the 1964 Declaration of Helsinki.

Disclosure

The author(s) report no conflicts of interest in this work.

References

1. Aneja A, Luo TD, Liu B, et al. Anterolateral distal tibia locking plate osteosynthesis and their ability to capture OTAC3 pilon fragments. *Injury*. 2018;49(2):409–413. doi:10.1016/j.injury.2017.12.015
2. Bastias C, Lagos L. New principles in pilon fracture management: revisiting rüedi and allgöwer concepts. *Foot Ankle Clin*. 2020;25(4):505–521. doi:10.1016/j.fcl.2020.08.004
3. Zelle BA, Dang KH, Ornell SS. High-energy tibial pilon fractures: an instructional review. *Int Orthop*. 2019;43(8):1939–1950. doi:10.1007/s00264-019-04344-8
4. Assal M, Ray A, Stern R. Strategies for surgical approaches in open reduction internal fixation of pilon fractures. *J Orthop Trauma*. 2015;29 (2):69–79. doi:10.1097/BOT.0000000000000218
5. Topliss CJ, Jackson M, Atkins RM. Anatomy of pilon fractures of the distal tibia. *J Bone Joint Surg Br*. 2005;87(5):692–697. doi:10.1302/0301-620X.87B5.15982
6. Cole PA, Mehrle RK, Bhandari M, Zlowodzki M. The pilon map: fracture lines and comminution zones in OTA/AO type 43C3 pilon fractures. *J Orthop Trauma*. 2013;27(7):e152–e156. doi:10.1097/BOT.0b013e318288a7e9
7. Rüedi T. Frakturen des Pilon Tibial: Ergebnisse nach 9 Jahren [Intraarticular fractures of distal tibia: results after 9 years (author's transl)]. *Arch Orthop Unfallchir*. 1973;76(4):248–254. German. doi:10.1007/BF00416372
8. Leonetti D, Tigani D. Pilon fractures: a new classification system based on CT-scan. *Injury*. 2017;48(10):2311–2317. doi:10.1016/j.injury.2017.07.026
9. Saini R, Sharma A, Sidhu SS, et al. Tibia. *J Orthop Trauma*. 2018;32(1):S49–S60. doi:10.1097/BOT.0000000000001074
10. Herscovici D, Sanders RW, Infante A, et al. Bohler incision: an extensile anterolateral approach to the foot and ankle. *J Orthop Trauma*. 2000;14 (6):429–432. doi:10.1097/00005131-200008000-00009
11. Teeny SM, Wiss DA. Open reduction and internal fixation of tibial plafond fractures. Variables contributing to poor results and complications. *Clin Orthop Relat Res*. 1993;292:108–117.
12. Korkmaz A, Ciftdemir M, Ozcan M, Copuroğlu C, Sarıdoğan K. The analysis of the variables, affecting outcome in surgically treated tibia pilon fractured patients. *Injury*. 2013;44(10):1270–1274. doi:10.1016/j.injury.2013.06.016
13. Flores M, Ciminero M, Kottmeier SA, Botros D, Zelle BA, Shearer DW. Pilon fractures: consensus and controversy. *OTA Int*. 2023;6(3 Suppl): e236. doi:10.1097/OI9.0000000000000236
14. Tang X, Tang PF, Wang MY, et al. Pilon fractures: a new classification and therapeutic strategies. *Chin Med J*. 2012;125(14):2487–2492.
15. Chen H, Cui X, Ma B, Rui Y, Li H. Staged procedure protocol based on the four-column concept in the treatment of AO/OTA type 43-C3.3 pilon fractures. *J Int Med Res*. 2019;47(5):2045–2055. doi:10.1177/0300060519836512
16. Zhang J, Wang H, Pen C, et al. Characteristics and proposed classification system of posterior pilon fractures. *Medicine*. 2019;98(3):e14133. doi:10.1097/MD.0000000000014133
17. Bakan ÖM, Vahabi A, Özkayın N. Management of complex pilon fractures: is it necessary to fix all the columns in AO/OTA type 43-C fractures? *Injury*. 2023;54(12):111153. doi:10.1016/j.injury.2023.111153
18. Sohn HS, Oh JK, Yang HS, Kim HR. Anatomically precontoured locked plates in pilon fractures: a computed tomography based and cadaveric study. *Indian J Orthop*. 2018;52(6):665–671. doi:10.4103/ortho.IJOrtho_602_16
19. Mason LW, Marlow WJ, Widnall J, et al. Pathoanatomy and associated injuries of posterior malleolus fracture of the ankle. *Foot Ankle Int*. 2017;38 (11):1229–1235. doi:10.1177/1071100717719533

20. Vosoughi AR, Jayatilaka MLT, Fischer B, et al. CT analysis of the posteromedial fragment of the posterior malleolar fracture. *Foot Ankle Int*. 2019;40(6):648–655. doi:10.1177/1071100719830999
21. Haraguchi N, Armiger RS. Mechanism of posterior malleolar fracture of the ankle: a cadaveric study. *OTA Int*. 2020;3(2):e060. doi:10.1097/OI9.0000000000000060
22. Mehta S, Gardner MJ, Barei DP, Benirschke SK, Nork SE. Reduction strategies through the anterolateral exposure for fixation of type B and C pilon fractures. *J Orthop Trauma*. 2011;25:116–122. doi:10.1097/BOT.0b013e3181cf00f3